JOURNAL OF ELECTROMAGNETIC ENGINEERING AND SCIENCE, VOL. 24, NO. 1, 89~97, JAN. 2024

https://doi.org/10.26866/jees.2024.1.r.208
ISSN 2671-7263 (Online) · ISSN 2671-7255 (Print)

# A Compact MIMO Antenna Design Using the Wideband Ground-Radiation Technique for 5G Terminals

Rui Li[1] · Longyue Qu[2,3] · Hyeongdong Kim[1,*]

## Abstract

This paper introduces a 4 × 4 multiple-input and multiple-output (MIMO) antenna application based on the conception of the characteristic mode of 5G terminals. The proposed antenna used a series capacitor and a parallel capacitor to control input impedance matching, while the resonance frequency was controlled by employing a resonance loop capacitor. In this way, we achieved a compact miniaturization antenna that uses ground radiation for the target 5G New Radio (NR) operating bands with n48, n77, and n78 bands. The simulation and measurement data revealed that the −6 dB bandwidth of the proposed antenna was approximately 1,240 MHz (ranging from 3.14 GHz to 4.38 GHz), while the efficiency also improved from 38.7% (reference) to 49.1% (proposed) within the 3 GHz to 4.6 GHz range. Furthermore, the radiation pattern exhibited satisfactory radiation performance. Therefore, it was concluded that the proposed 4 × 4 MIMO antenna set technology has promising prospects for application in 5G communication terminals in the future.

**Key Words**: Characteristic Mode, Ground Radiation, Isolation, Input Impedance, MIMO Antenna, 5G System.

## I. Introduction

With the rapid development of mobile communication technology, compact miniaturized antennas are currently being used in a wide range of applications. In particular, the development of 5G telecommunication systems for mobile handsets has massively increased the demand for high data quality and data transfer rates. As a result, designing antennas that support wide band requirements, even when the technology is miniaturized, has emerged as a challenge [1–4].

To address this issue, multiple-input and multiple-output (MIMO) antenna systems that can transmit and receive signals are being used globally. Notably, these systems can be of great use in 5G MIMO communications. Today, the integration of more antennas into communication terminals has become a megatrend. In this regard, the MIMO antenna offers the advantages of improved space utilization and increased coverage of wireless systems [5]. Specifically, in the context of the sub-6 GHz band, the 3.5 GHz (3.4–3.6 GHz) and New Radio (NR) operating bands within the FR1 band have attracted a wide range of applications for 5G wireless communication in recent years [6, 7]. In this context, while the characteristic mode theory was revised by Garbacz in 1968, the theory of characteristic modes for conducting bodies was revised by Harrington and Mautz in 1971 [8].

Manuscript received February 20, 2023 ; Revised May 22, 2023 ; Accepted August 31, 2023. (ID No. 20230220-037J)
[1]Department of Electronics and Computer Engineering, Hanyang University, Seoul, Republic of Korea.
[2]Department of Electronics and Information Engineering, Harbin Institute of Technology (Shenzhen), Shenzhen, China.
[3]Guangdong Provincial Key Laboratory of Aerospace Communication and Networking Technology, Harbin Institute of Technology (Shenzhen), Shenzhen, China.
[*]Corresponding Author: Hyeongdong Kim (e-mail: hdkim@hanyang.ac.kr)
Rui Li and Longyue Qu contributed equally to this work.

This concept has greatly affected MIMO antenna design that is aimed at improving correlation performance and isolation between antennas [9–13]. Consequently, developing a compact and efficient MIMO antenna was found to be the primary focus of many studies. However, in previous studies [14, 15], the antenna clearance regions (more than 10 mm × 10 mm) took up a significant amount of physical space on the printed circuit board (PCB), making the process of antenna miniaturization difficult. Nonetheless, ground-radiation antennas using small clearance technology have already been applied in many devices [16–19]. In this paper, the researchers combined the proposed antenna feed structure with ground radiation technology designed for 5G terminal equipment.

Specifically, this paper proposes a 4 × 4 MIMO antenna based on the concept of the characteristic mode for 5G terminals [12]. The proposed feeding structure includes a series capacitor and a parallel capacitor to control the antenna input impedance matching for the proposed MIMO antenna system. Furthermore, a resonance loop capacitor is employed to control the resonance frequency of the proposed antenna. Moreover, an antenna using ground radiation to achieve wide-band technology was designed. The proposed antenna attained a –6 dB bandwidth of 1,240 MHz, ranging from 3.14 GHz to 4.38 GHz, in the simulation, while the measurement results showed a satisfactory performance of 1,380 MHz for a –6 dB bandwidth, with frequencies ranging from 3.12 GHz to 4.50 GHz. Additionally, the average efficiency increased from 38.7% (reference) to 49.1% (proposed) in the 3 GHz–4.6 GHz range. The target frequency of the proposed technology was 3.3 GHz to 4.2 GHz, meaning that it could operate in the 5G NR n48 (3,550–3,700 MHz), n77 (3,300–4,200 MHz), and n78 (3,300–3,800 MHz) platforms. These results indicate that the proposed technology has good application prospects for 5G communication terminal antenna designs.

## II. Antenna Design and Characteristic Mode Analysis

The proposed 4 × 4 MIMO antenna system for the 3–4.5 GHz frequency range with n48, n77, and n78 applications is depicted in Fig. 1. The 50 mm × 120 mm × 1 mm ground plane is printed on an FR4 (frame retardant type 4) substrate with a dielectric constant of $\varepsilon_r = 4.4$. Each proposed antenna, with a ground clearance of 5 mm × 4 mm, is identical, mirror-symmetric, and located 24 mm from the edge on top of the PCB.

This study considers a traditional ground-radiation antenna as the reference antenna, where the magnetic flux produced by a loop-type current around the clearance, which is the resonance frequency, was determined by the chip capacitor $C_g$. Meanwhile, the input impedance matching in the reference antenna was determined by the chip capacitor $C_a$, as shown in Fig. 1(b) [16–19]. For comparison purposes, a voltage source was added for the excitation of the reference antenna while a series capacitor $C_g$ (0.15 pF), which adjusted its resonance frequency when excited by a 2.5 mm × 2.5 mm feeding loop [16–19], was added in series with capacitor $C_a$ (0.35 pF) for impedance matching, as shown in Fig. 1(b). The edge-to-edge separation between ANT1 and ANT2, as well as between ANT3 and ANT4, is 64 mm (0.87λ).

Meanwhile, the proposed antenna was designed on a 5 mm × 4 mm clearance of the ground plane. Furthermore, a resonance capacitor $C_r$ (0.15 pF) was added at the end of the clearance to control the antenna's resonance frequency. A 2.5 mm × 2.1 mm feeding structure was employed for the proposed antenna, equipped with a series capacitor $C_f$ (0.51 pF) and a parallel capacitor $C_s$ (0.38 pF) to achieve input impedance matching, as shown in Fig. 1(c) [20]. Moreover, the proposed antenna had a different feeding structure than the traditional ground-radiation antenna. In this context, it should be noted that the conductor line widths for both the reference and proposed MIMO antennas were 0.5 mm. It is also worth noting that the proposed MIMO technology can be applied to different situations as well, including for the purpose of accommodating various sizes and modules of the evaluation board and for different size changes in feed structures.

## III. Simulation Results and Operation Mechanism

The simulation results obtained for the scattering parameters

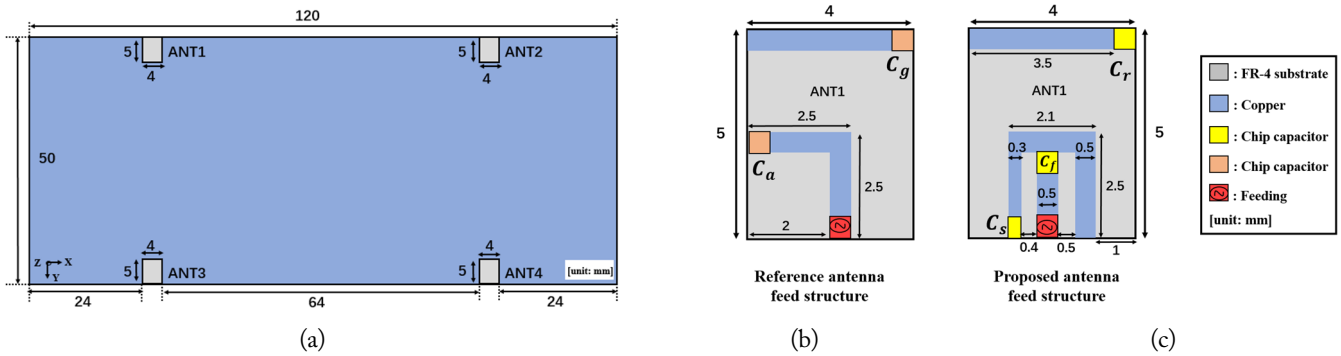


(a) (b) (c)

Fig. 1. Geometries of (a) the MIMO antenna ground plane, (b) detailed dimensions of the reference antenna element, and (c) detailed dimensions of the proposed antenna element.

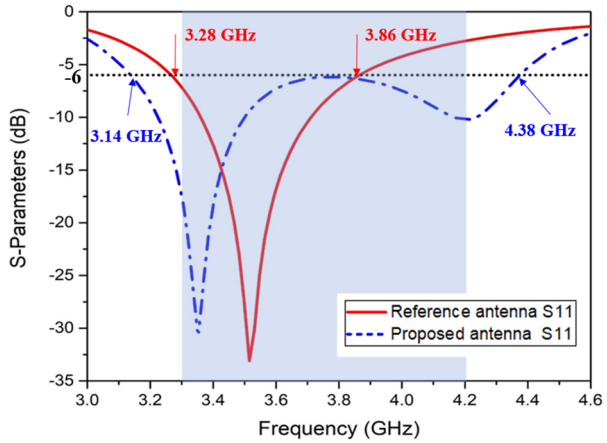


Fig. 2. Simulated *S*-parameters of the reference and proposed 4 × 4 MIMO antennas.

(*S*-parameters) of the reference and proposed MIMO antennas are presented in Fig. 2. The –6 dB bandwidth corresponds to the voltage stand wave ratio (VSWR) of 3, which is widely used, although a VSWR of 2 (–9.54 dB bandwidth) is also used in some cases [21, 22]. Fig. 2 shows that a –6 dB bandwidth of 600 MHz (ranging from 3.27 GHz to 3.87 GHz) was achieved by reference ANT1, while the proposed ANT1 attained a –6 dB bandwidth of 1,240 MHz (ranging from 3.14 GHz to 4.38 GHz), which covers the target frequency band (from 3.3 GHz to 4.2 GHz) for 5G applications entirely. Fig. 3 shows the simulated proposed antenna $S_{11}$ values along with variations in the capacitor $C_r$ values to illustrate the operation principle of the proposed antenna using ground radiation. It is evident that the central resonance frequency decreases as the capacitor $C_r$ increases to 0.2 pF ($C_f$ = 0.51 pF, $C_s$ = 0.38 pF remained unchanged). This effect can be attributed to the inductance between the transmission line and ground plane, with the loaded capacitor $C_r$ forming a loop-type resonance circuit using ground radiation [23]. This indicates that with an increase in the capacitance of $C_r$, the loop resonance frequency decreases. Furthermore, the inductance increases along with an increase in antenna clearance, causing the resonance frequency to decrease.

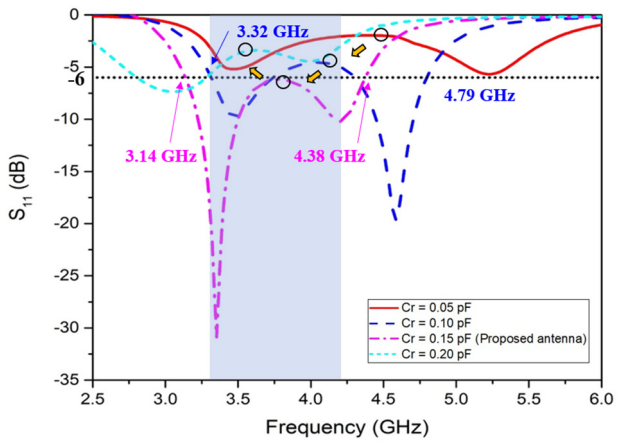


Fig. 3. Simulated $S_{11}$ with variation of capacitor $C_r$ for the proposed ANT1.

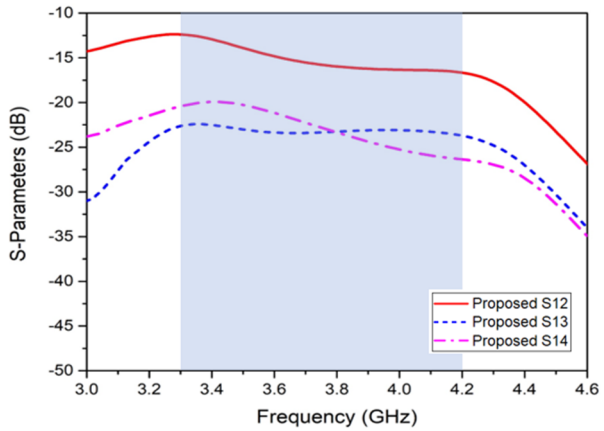


Fig. 4. Simulated *S*-parameters of the proposed 4 × 4 MIMO antenna.

Therefore, the resonance frequency can not only be controlled by adjusting the capacitor value, but also by changing the clearance area. The simulated *S*-parameters of isolation for ANT1 to ANT4 are shown in Fig. 4, where it can be observed that the mutual coupling $S_{12}$ between the proposed ANT1 and ANT2 is lower than –12.4 dB over the target frequency band. Meanwhile, for the other antennas, mutual coupling $S_{13}$ and $S_{14}$ is lower than –22.4 dB and –19.9 dB, respectively, over the target frequency band. To conduct a better interpretation of the operation mechanism of the proposed 4 × 4 MIMO antenna system, the simulated surface current distribution at 3.5 GHz for ANT1 is shown in Fig. 5(a), which clearly exhibits the operating current modes. Two loop currents are found in the feeding structure, denoted as Loop 1 and Loop 2, which can be represented by a two-pot impedance $[Z]$ matrix [24], as follows:

$$[Z] = \begin{bmatrix} j\left(\omega L_{Loop1} - \frac{1}{\omega C_f}\right) & j\omega L_{Loop1} \\ j\omega L_{Loop1} & j\left(\omega L_{Loop2} - \frac{1}{\omega C_s}\right) \end{bmatrix}, \quad (1)$$

where $L_{Loop1}$ and $L_{Loop2}$ refer to the inductances of Loop 1 and Loop 2 in the feeding structure, respectively. The ground plane was modeled as a series RLC circuit consisting of $R_g$, $L_g$, and $C_g$ as a circuit model for the antenna elements, as shown in Fig. 5(b). The circuit between the ground plane and the proposed antenna impedance matching, using $Z_{11}$, $Z_{12}$, and $Z_{22}$ in the two-port network, can be expressed as follows [19]:

$$Z_{in} = Z_{11} - \frac{{Z_{12}}^2}{Z_{22}} \quad (2)$$

$$Z_{11} = j\left(\omega L_{feed} - \frac{1}{\omega(C_f + C_s)}\right) \quad (3)$$

$$Z_{12} = (\omega L_{feed})^2 \quad (4)$$

$$Z_{22} = R_r + R_g + j\left(\omega(L_{feed} + L_r + L_g) - \frac{1}{\omega(C_r + C_g)}\right) \quad (5)$$

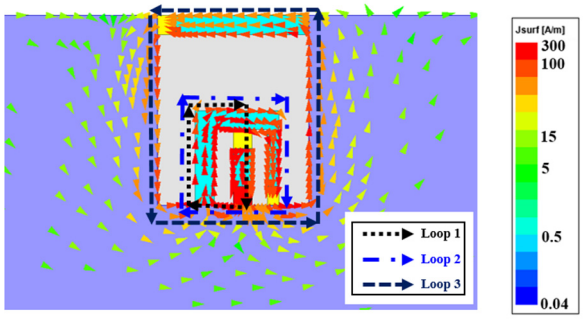


(a)

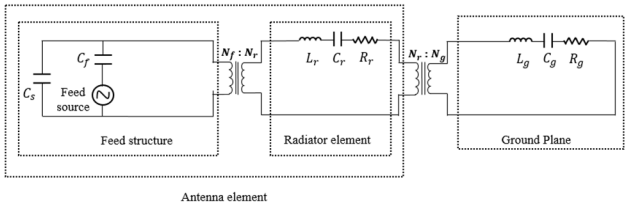


(b)

Fig. 5. (a) Simulated surface current distributions of the ground radiation in the proposed ANT1 at 3.5 GHz when excited by the feed structure. (b) Diagrammatic sketch of the proposed antenna structure, resonance loop (radiator element), and ground plane.

In Eqs. (2)–(5), $Z_{11}$ denotes the feed structure network input impedance, $Z_{12}$ refers to the mutual input impedance between the feed structure and the ground plane, and $Z_{12}$ is the input impedance of both the outside resonance loop and the ground plane. Furthermore, $L_{feed}$ indicates the inductance, with the feed structure including $L_{Loop1}$ and $L_{Loop2}$, while $R_r$ and $L_r$ are the resistance and inductance of the outside resonance loop.

In conclusion, the proposed antenna is a small loop-type antenna forming a dipole-type radiator that can excite the ground plane [25]. According to the reaction concept and the characteristic modes theory of conducting bodies, the coupling between the ground plane and the proposed antenna can be expressed using the modal excitation coefficient [24] as follows:

$$\langle \bar{E}^g, \bar{J}^p \rangle = \iiint \bar{E}^g \cdot \bar{J}^p \, d\tau, \tag{6}$$

$$\langle \bar{H}^g, \bar{M}^p \rangle = -\iiint \bar{H}^g \cdot \bar{M}^p \, d\tau, \tag{7}$$

$$\bar{J} = \sum n \frac{\langle \bar{E}^g, \bar{J}^p \rangle}{1 + j\lambda_n} \bar{J}_n, \tag{8}$$

where $\bar{E}^g$ and $\bar{H}^g$ are the electric fields and magnetic fields generated from the ground plane with characteristic modes, and $\bar{J}^p$ and $\bar{M}^p$ are the electric currents and magnetic currents produced by the antenna in Eqs. (6) and (7). The loop-type current mode $\bar{M}^p$ can react with the ground plane characteristic magnetic field $\bar{H}^g$. The total current $\bar{J}$ on the ground plane can be expressed by Eq. (8), where $\lambda_n$ is the eigenvalue associated with $\bar{J}_n$, which is the $n$th characteristic current mode [8]. When $\lambda_n$ is infinitely close to 0, the denominator term becomes smaller at the same time that the coupling performance maximizes. In this regime, the characteristic modes of the ground plane radiate effectively in resonance [12]. Consequently, the antenna is coupled with the characteristic mode of the ground plane, where a resonance close to the target operating frequency achieves better radiation performance. Fig. 6 shows the simulated surface current distribution at 3.5 GHz for the proposed MIMO antenna system with Port 1 excitation. ANT1 excites the PCB at 1.5 times the wavelength of the mode, ensuring good performance of the antenna [10].

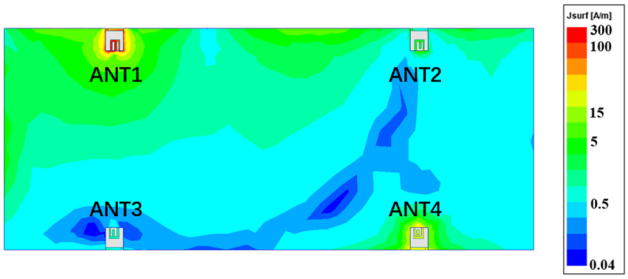


Fig. 6. Simulated surface current distribution of the 4 × 4 MIMO antenna system at 3.5 GHz with Port 1 excitation.

## IV. Experimental Results

The 4 × 4 MIMO reference and proposed antennas were fabricated and measured using Agilent 8753ES network analyzers in a 6 m × 3 m × 3 m 3D CITA OTA chamber, as shown in Fig. 7. For input impedance matching, the feed structure series capacitor $C_a$ and the resonance loop series capacitor $C_g$ were set to 0.5 pF and 0.2 pF, respectively, for the reference antenna. Meanwhile, for the proposed antenna, the series capacitor $C_g$, the parallel capacitor $C_s$, and the resonance loop capacitor $C_r$ were set to 0.4 pF, 0.25 pF, and 0.2 pF, respectively. The reflection coefficients presented in Fig. 8 show that a –6 dB bandwidth of 580 MHz (3.28 GHz–3.86 GHz) and 1,380 MHz (3.12 GHz–4.50 GHz) are obtained for the reference antenna and the proposed antenna, respectively. Furthermore, Fig. 9 shows the measured total efficiency data on average, where the reference ANT1 is at 38.7% and the proposed ANT1 is at 49.1% within the 3 GHz to 4.6 GHz range. The measurement results of mutual coupling between ANT1 and ANT4 of the proposed antenna are both lower

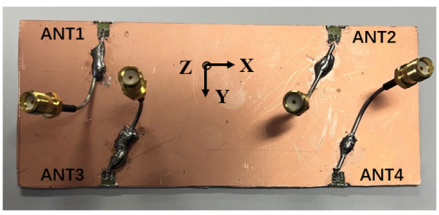


Fig. 7. Fabricated 4 × 4 MIMO antenna prototype.

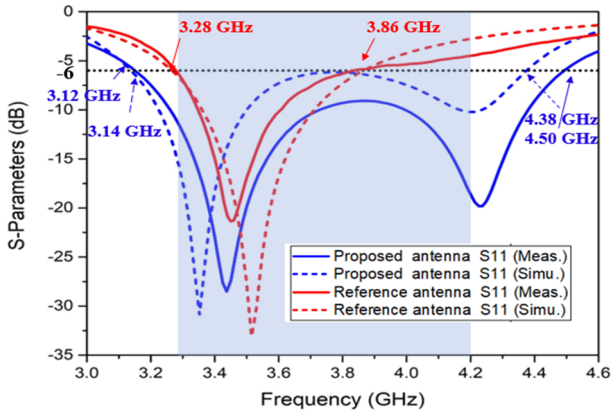


Fig. 8. Simulated and measured reflection coefficients of the reference and proposed antennas.

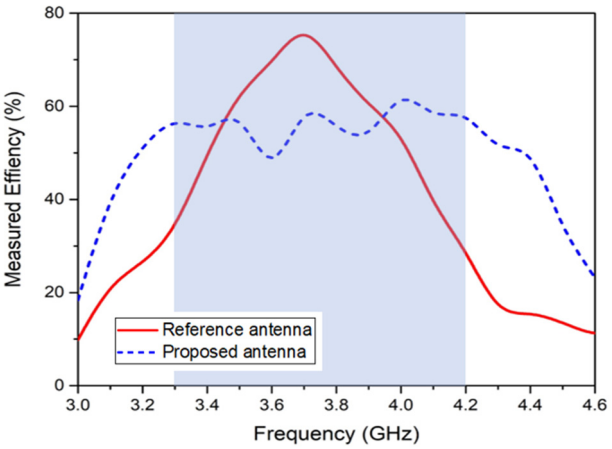


Fig. 9. Measured total efficiency of reference ANT1 and proposed ANT1.

than –15 dB, indicating characteristics that are similar to the simulation results, as shown in Fig. 10. Furthermore, the measured envelope correlation coefficient (ECC), derived from far-field 3D radiation patterns, is shown in Fig. 11. It is observed that all measured ECC values are below 0.2 in the target frequency band of

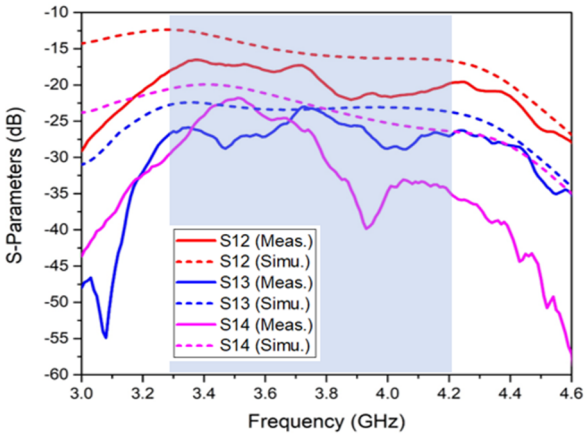


Fig. 10. Simulated and measured *S*-parameters of the proposed 4 × 4 MIMO antennas.

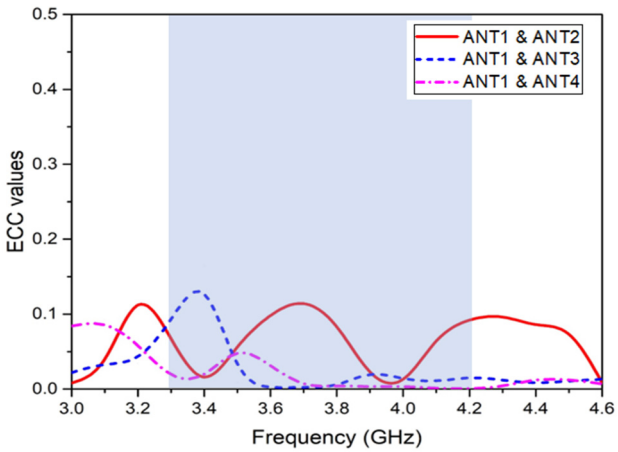


Fig. 11. Measured ECC values of the fabricated 4 × 4 MIMO antennas.

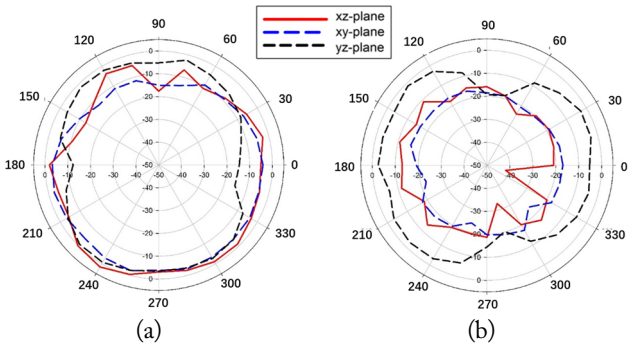


Fig. 12. Measured far-field omnidirectional radiation patterns of the proposed antenna at 3.5 GHz: (a) $E_\theta$ and (b) $E_\varphi$.

3.3 GHz to 4.2 GHz, which is significantly lower than the acceptable threshold of 0.5. This highlights that the proposed 4 × 4 MIMO antenna offers good diversity performance in the operating frequency band. Fig. 12 illustrates the radiation patterns of the proposed antenna at 3.5 GHz, with the far-field theta and phi directions showing good omnidirectional performance. These measurement results highlight that the proposed technology exhibits a wider bandwidth and better performance than the reference antenna.

## V. Further Study and Discussion

Previous studies have shown that if an antenna is located at the maximum current position on the ground plane, it exhibits good performance [12]. In general, in a MIMO antenna design, an isolator is used to reduce the isolation of the antenna and, in turn, to decrease interference to improve antenna performance [26]. The operation mechanism of the proposed MIMO antenna at 3.75 GHz is shown in Fig. 13. The length of the proposed antenna's PCB is 120 mm (about 1.5λ), with the antenna set located in positions with maximum current distribution [12]. The results show that all the proposed antenna sets exhibit good antenna perfor-

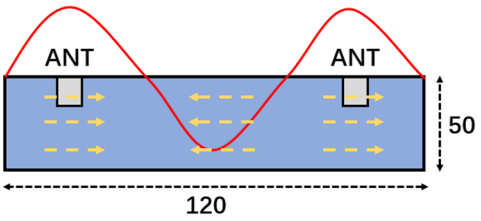


Fig. 13. Operation mechanism of the proposed MIMO antenna set at 3.75 GHz.

mance.

In this context, since two sides of 5G mobile terminal equipment are primarily used in low-frequency antenna design (0.69–0.96 GHz and 1.69–2.69 GHz), adding more antennas to one side of the device has become increasingly challenging. Furthermore, with the increasing demand for data transmission on mobile devices, integrating more antennas into these devices has emerged as a trend [23]. Moreover, previous studies did not use the ground-radiation antenna for exploring the design of an $n \times n$ MIMO antenna. In this case, since no additional structure is used to reduce isolation in this study, one could add a set of antennas to the proposed antenna to construct a 6 × 6 MIMO antenna using the current distribution.

The design of the proposed 6 × 6 MIMO antenna system is shown in Fig. 14. Notably, the design for ANT1 to ANT4 in this antenna is the same as the 4 × 4 MIMO antenna set. Moreover, the ANT5 and ANT6 structures are the same as those of ANT1 and ANT3, thus maintaining mirror symmetry.

The *S*-parameters of the proposed 6 × 6 MIMO antenna are presented in Fig. 15, showing that the proposed $S_{11}$ and $S_{55}$ achieve a bandwidth of 1,180 MHz (ranging from 3.18 GHz to 4.36 GHz) and 1,070 MHz (ranging from 3.26 GHz to 4.33 GHz), respectively, under the –6 dB bandwidth, thus covering the target frequency band (3.3 GHz to 4.2 GHz). Both the simulation and measurement results for the proposed structure point to an $S_{11}$ of 12,900 MHz (ranging from 3.21 GHz to 4.50 GHz) and an $S_{55}$ of 1440 MHz (ranging from 3.22 GHz to 4.66 GHz) under the –6 dB bandwidth, which also covers the target frequency band. Furthermore, the simulated results of the isolation performance between the two antenna elements of the MIMO

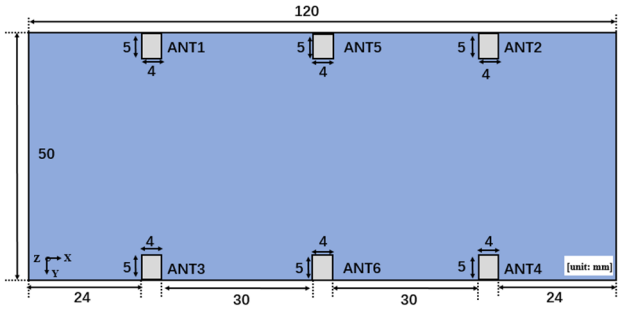


Fig. 14. Geometry of the 6 × 6 MIMO antenna ground plane.

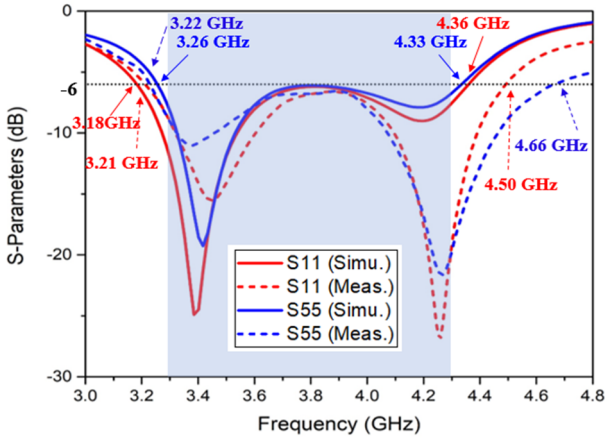


Fig. 15. Simulated and measured reflection coefficients of the 6 × 6 MIMO antenna.

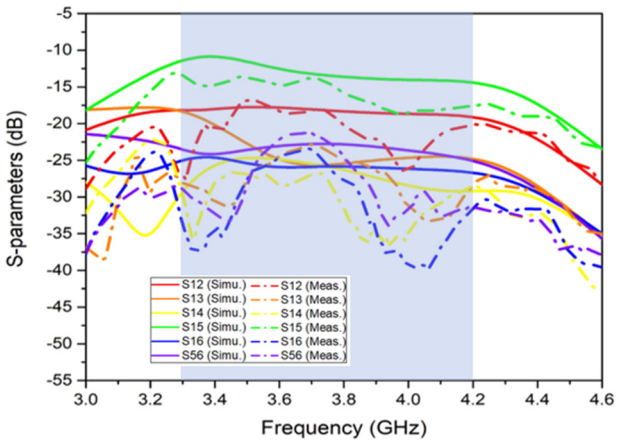


Fig. 16. Simulated and measured S-parameters of the 6 × 6 MIMO antenna.

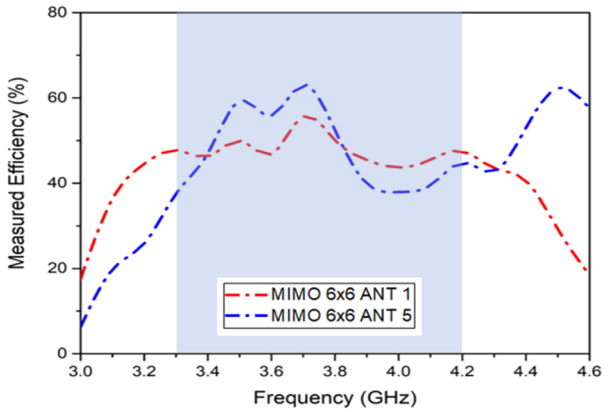


Fig. 17. Measured total efficiency of the 6 × 6 MIMO ANT1 and ANT5.

antenna set is over 10.9 dB, demonstrating good isolation between the proposed antennas. Meanwhile, the measurement results show that the isolation between two antenna elements in the MIMO antenna set is over 13.1 dB for the proposed antennas, as shown in Fig. 16. Fig. 17 illustrates the measurement results

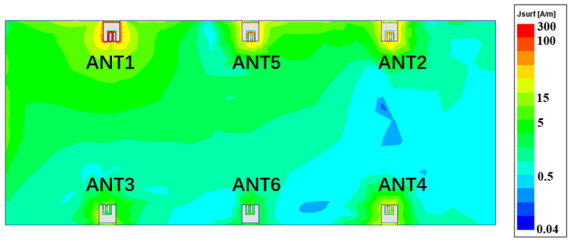


Fig. 18. Simulated surface current distribution of the 6 × 6 MIMO antenna system at 3.5 GHz with Port 1 excitation.

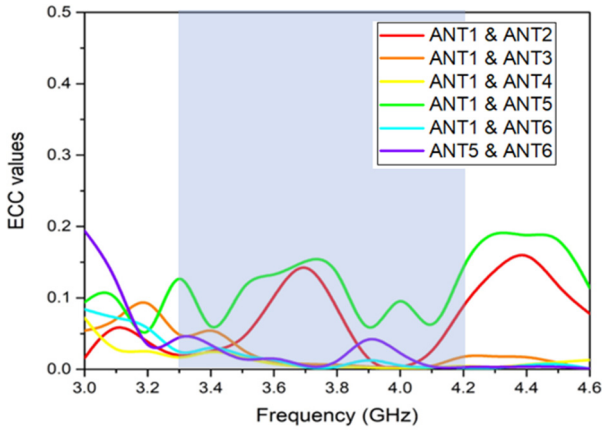


Fig. 19. Measured ECC values of the fabricated 6 × 6 MIMO antennas.

of the total efficiency data on average for the 6 × 6 MIMO antenna, where ANT1 is at 42.0% and ANT5 at 44.1% in the 3 GHz to 4.6 GHz range. The simulated surface current distribution at 3.5 GHz in the proposed 6 × 6 MIMO antenna system with Port 1 excitation is shown in Fig. 18. Furthermore, the measurement ECC results derived from the far-field 3D radiation patterns are shown in Fig. 19, where it is observed that all measured ECC values are below 0.2 in the target frequency band from 3.3 GHz to 4.2 GHz.

The simulated and measurement results demonstrate that the MIMO antenna can be designed without using isolators. Even without isolators, the current distribution used to select the antenna area maintained good isolation between the antenna elements while also achieving satisfactory bandwidth and performance. Further experimentation revealed that more antennas could be integrated into this structure through current distribution in the mobile device without the need for any additional structure. This method can be used as a reference when designing an antenna for mobile devices in the future. Table 1 compares the results of the proposed antenna with those attained in previous studies in terms of antenna size, bandwidth, efficiency, operating frequency band, and antenna type [5, 11, 17, 21, 23]. The comparison clearly indicates that the proposed antenna has a wider bandwidth than other antennas of the same type in the same operating frequency band. In addition, in contrast to previous studies, the proposed antenna offers the advantage of easy manipulation of impedance matching.

## VI. Conclusion

This paper introduces a 4 × 4 MIMO antenna application based on the concept of the characteristic mode for 5G terminals. The proposed antenna uses a series and parallel capacitor feed structure to control input impedance matching while also employing ground radiation to achieve a –6 dB bandwidth of approximately 1,240 MHz (ranging from 3.14 GHz to 4.38 GHz) in the simulation and 1,380 MHz (ranging from 3.12 GHz to 4.50 GHz) in the measurement results. Furthermore, the experimental measurements of the proposed antenna demonstrated satisfactory efficiency, which increased from 38.7% (reference) to 49.1% (proposed), indicating good antenna performance. Moreover, the 6 × 6 MIMO antenna design using current distribution also exhibited satisfactory bandwidth and good antenna performance. Therefore, it is concluded that the proposed technology will have good application prospects for 5G communication terminals in the future.

This study was supported by the National Research Foundation of Korea through a grant from the Korean government (Ministry of Science and ICT) (No. 2019R1F1A1063993).

## References

[1] J. N. Lee, S. B. Hyun, and Y. K. Cho, "A compact ultra-wideband chip antenna with bandwidth extension patch and sim-

Table 1. Comparison results of the proposed antenna with those in the reference literature

| Study | Overall size (mm) | BW (MHz) | Antenna average efficiency (%) | Operating frequency (GHz) | Antenna type |
|---|---|---|---|---|---|
| Deng et al. [5] | 70 × 140 × 1 | 420 (-6 dB) | 51 | 3.4–3.6 | IFA |
| Zahid et al. [11] | 45 × 45 × 2 | 100 (-6 dB) | 65 | 2.4–2.5 | Loop |
| Liu et al. [17] | 15 × 50 × 1 | 310 (-10 dB) | 70 | 2.4–2.5 | Loop |
| Piao et al. [23] | 140 × 70 × 1 | 430 (-6 dB) | 56 | 3.4–3.6 | Loop |
| Lee et al. [21] | 60 × 115 × 1 | 520 / 610 (-6 dB) | 33.45 / 45.71 | 0.7–1.4 / 1.7–2.2 | IFA |
| Proposed | 120 × 50 × 1 | 1,240 (-6 dB) | 49 | 3.0–4.6 | Loop |

ple isolator for MIMO systems for mobile handheld terminals," *Journal of Electromagnetic Engineering and Science*, vol. 22, no. 3, pp. 272-282, 2022. https://doi.org/10.26866/jees.2022.3.r.87

[2] G. Dong, J. Huang, S. Lin, Z. Chen, and G. Liu, "A compact dual-band MIMO antenna for sub-6 GHz 5G terminals," *Journal of Electromagnetic Engineering and Science*, vol. 22, no. 5, pp. 599-607, 2022. https://doi.org/10.26866/jees.2022.5.r.128

[3] P. Shanmugam, "Design and analysis of a frequency reconfigurable penta-band antenna for WLAN and 5G applications," *Journal of Electromagnetic Engineering and Science*, vol. 21, no. 3, pp. 228-235, 2021. https://doi.org/10.26866/jees.2021.3.r.30

[4] I. Kim and B. Lee, "Wideband antenna for high-frequency 5G wireless communication," *Journal of Electromagnetic Engineering and Science*, vol. 22, no. 3, pp. 296-301, 2022. https://doi.org/10.26866/jees.2022.3.r.90

[5] C. Deng, D. Liu, and X. Lv, "Tightly arranged four-element MIMO antennas for 5G mobile terminals," *IEEE Transactions on Antennas and Propagation*, vol. 67, no. 10, pp. 6353-6361, 2019. https://doi.org/10.1109/TAP.2019.2922757

[6] M. Y. Li, Y. L. Ban, Z. Q. Xu, J. Guo, and Z. F. Yu, "Tri-polarized 12-antenna MIMO array for future 5G smartphone applications," *IEEE Access*, vol. 6, pp. 6160-6170, 2017. https://doi.org/10.1109/ACCESS.2017.2781705

[7] Y. Li, Y. Luo, and G. Yang, "Multiband 10-antenna array for sub-6 GHz MIMO applications in 5-G smartphones," *IEEE Access*, vol. 6, pp. 28041-28053, 2018. https://doi.org/10.1109/ACCESS.2018.2838337

[8] R. Harrington and J. Mautz, "Theory of characteristic modes for conducting bodies," *IEEE Transactions on Antennas and Propagation*, vol. 19, no. 5, pp. 622-628, 1971. https://doi.org/10.1109/TAP.1971.1139999

[9] J. Kim, L. Qu, H. Jo, R. Zhang, and H. Kim, "A MIMO antenna design based on the characteristic mode," *Microwave and Optical Technology Letters*, vol. 59, no. 4, pp. 893-898, 2017. https://doi.org/10.1002/mop.30429

[10] J. Won, S. Jeon, and S. Nam, "Identifying the appropriate position on the ground plane for MIMO antennas using characteristic mode analysis," *Journal of Electromagnetic Engineering and Science*, vol. 16, no. 2, pp. 119-125, 2016. https://doi.org/10.5515/JKIEES.2016.16.2.119

[11] Z. Zahid, L. Qu, and H. H. Kim, "Circularly polarized loop-type ground radiation antenna for IoT applications," *Journal of Electromagnetic Engineering and Science*, vol. 19, no. 3, pp. 153-158, 2019. https://doi.org/10.26866/jees.2019.19.3.153

[12] H. Lee, Z. Zahid, and H. Kim, "Loop-type ground radiation antenna for a C-shaped ground plane," *Journal of Electromagnetic Engineering and Science*, vol. 19, no. 1, pp. 1-5, 2019. https://doi.org/10.26866/jees.2019.19.1.1

[13] B. R. Perli and M. R. Avula, "Design of wideband elliptical ring monopole antenna using characteristic mode analysis," *Journal of Electromagnetic Engineering and Science*, vol. 21, no. 4, pp. 299-306, 2021. https://doi.org/10.26866/jees.2021.4.r.37

[14] Z. Qin, W. Geyi, M. Zhang, and J. Wang, "Printed eight-element MIMO system for compact and thin 5G mobile handest," *Electronics Letters*, vol. 52, no. 6, pp. 416-418, 2016. https://doi.org/10.1049/el.2015.3960

[15] Y. L. Ban, C. Li, G. Wu, and K. L. Wong, "4G/5G multiple antennas for future multi-mode smartphone applications," *IEEE Access*, vol. 4, pp. 2981-2988, 2016. https://doi.org/10.1109/ACCESS.2016.2582786

[16] Y. Liu, X. Lu, H. Jang, H. Choi, K. Jung, and H. Kim, "Loop-type ground antenna using resonated loop feeding, intended for mobile devices," *Electronics Letters*, vol. 47, no. 7, pp. 426-427, 2011. https://doi.org/10.1049/el.2011.0094

[17] Y. Liu, J. Lee, H. H. Kim, and H. Kim, "Ground radiation method using slot with coupling capacitors," *Electronics Letters*, vol. 49, no. 7, pp. 447-448, 2013. https://doi.org/10.1049/el.2012.4520

[18] Y. Liu, H. H. Kim, and H. Kim, "Loop-type ground radiation antenna for dual-band WLAN applications," *IEEE Transactions on Antennas and Propagation*, vol. 61, no. 9, pp. 4819-4823, 2013. https://doi.org/10.1109/TAP.2013.2267716

[19] L. Qu, R. Zhang, and H. Kim, "High-sensitivity ground radiation antenna system using an adjacent slot for Bluetooth headsets," *IEEE Transactions on Antennas and Propagation*, vol. 63, no. 12, pp. 5903-5907, 2015. https://doi.org/10.1109/TAP.2015.2481919

[20] S. Jeon and H. Kim, "Mobile terminal antenna using a planar inverted-e feed structure for enhanced impedance bandwidth," *Microwave and Optical Technology Letters*, vol. 54, no. 9, pp. 2133-2139, 2012. https://doi.org/10.1002/mop.27035

[21] W. Lee, M. Park, and T. Son, "Hybrid MIMO antenna using interconnection tie for eight-band mobile handsets," *Journal of Electromagnetic Engineering and Science*, vol. 15, no. 3, pp. 185-193, 2015. https://doi.org/10.5515/JKIEES.2015.15.3.185

[22] X. Zhao, K. Kwon, and J. Choi, "MIMO antenna using resonance of ground planes for 4G mobile application," *Journal of Electromagnetic Engineering and Science*, vol. 13, no. 1, pp. 51-53, 2013. https://doi.org/10.5515/JKIEES.2013.13.1.51

[23] H. Piao, Y. Jin, and L. Qu, "A compact and straightforward self-decoupled MIMO antenna system for 5G applications," *IEEE Access*, vol. 8, pp. 129236-129245, 2020. https://doi.org/10.1109/ACCESS.2020.3008966

[24] F. M. Tesche, M. Ianoz, and T. Karlsson, *EMC Analysis Methods and Computational Models*. New York, NY: John Wiley & Sons, 1997.

[25] L. Qu, R. Zhang, and H. Kim, "Decoupling between ground radiation antennas with ground-coupled loop-type isolator for WLAN applications," *IET Microwaves, Antennas &*

*Propagation*, vol. 10, no. 5, pp. 546-552, 2016. https://doi.org/10.1049/iet-map.2015.0562

[26] H. Lee, J. Jeon, D. Park, H. Shin, and H. Kim, "MIMO antenna performance with isolator," *Microwave and Optical Technology Letters*, vol. 64, no. 5, pp. 946-952, 2022. https://doi.org/10.1002/mop.33212

Rui Li

https://orcid.org/0009-0009-1641-309X

received his B.S. degree in communication engineering from Yanbian University, Yanji, China. Since 2020, he has been pursuing an integrated Ph.D. in the Department of Electronics and Computer Engineering at Hanyang University, Seoul, Republic of Korea. His current research interests are MIMO, multi-wideband, high-efficiency, and mobile miniaturization antennas.

Longyue Qu

https://orcid.org/0000-0001-5152-091X

received his M.S. and Ph.D. degrees in electromagnetics and microwave engineering from Hanyang University, Seoul, Republic of Korea, in 2015 and 2018, respectively. He was a post-doctoral researcher at Hanyang University from September 2018 to August 2019, after which he was promoted to assistant research professor. He is the co-founder and CTO of Hanyang Antenna Design Co. Ltd., Shenzhen, China (2019 to 2022). Since 2022, he has been an assistant professor at the School of Electronics and Information Engineering, Harbin Institute of Technology, Shenzhen, China. Qu has authored over 50 articles and devised more than 30 inventions. He is a reviewer for several international journals and conferences. He is also an editorial board member of the *International Journal of Sensors, Wireless Communications, and Control*. His current research interests include antenna theory and design, metamaterial-based antenna technology, millimeter-wave arrays, and RF circuits. Qu was a recipient of the Korean Government Scholarship Award and the China Scholarship Council. His research earned a place in the Top 100 National R&D Excellence Award in 2015.

Hyeongdong Kim

https://orcid.org/0000-0003-4540-9451

received his B.S. and M.S. degrees from Seoul National University, Seoul, Republic of Korea, in 1984 and 1986, respectively, and his Ph.D. degree from the University of Texas in Austin in 1992. From May 1992 to February 1993, he was a post-doctoral fellow at the University of Texas in Austin. In 1993, he joined the Department of Electrical and Computer Engineering at Hanyang University, Seoul, Republic of Korea, as a professor. His current research interests include antenna theories and designs based on ground characteristic mode analysis, namely wideband, high-efficiency, circular polarization, MIMO, and high-sensitivity antennas.